Applied and Computational Harmonic Analysis **11**, 420–438 (2001)
doi:10.1006/acha.2001.0361, available online at http://www.idealibrary.com on IDEAL®

Design of Interpolating Biorthogonal Multiwavelet Systems with Compact Support

Jian-Kang Zhang,[1] Timothy N. Davidson, Zhi-Quan Luo, and K. Max Wong

Department of Electrical and Computer Engineering, McMaster University, Hamilton, Ontario, Canada
E-mail: davidson@mcmaster.ca, luozq@mcmaster.ca, and wongkm@mcmaster.ca

Communicated by P. P. Vaidyanathan

Received May 18, 2000; revised May 16, 2001

In this paper we characterize all totally interpolating biorthogonal finite impulse response (FIR) multifilter banks of multiplicity two, and provide a design framework for corresponding compactly supported multiwavelet systems with high approximation order. In these systems, each component of the analysis and synthesis portions possesses the interpolating property. The design framework is based on scalar filter banks, and examples with approximation order two and three are provided. We show that our multiwavelet systems preserve almost all of the desirable properties of the generalized interpolating scalar wavelet systems, including the dyadic-rational nature of the filter coefficients, equality of the flatness degree of the low-pass filters and the approximation order of the corresponding functions, and equality between the uniform samples of a signal and its projection coefficients for a given scale. This last property allows us to avoid the cumbersome prefiltering associated with standard multiwavelet systems. We also show that there are no symmetric totally interpolating biorthogonal multifilter banks of multiplicity two. Finally, we point out that our design framework incorporates a simple relationship between the multiscaling functions and multiwavelets that substantially simplifies the implementation of the system. © 2001 Academic Press

Key Words: multiwavelets; interpolation.

1. INTRODUCTION

Filter banks and wavelet transforms have become powerful tools in signal processing, image processing, communication systems, and many other related fields. The basic characteristic of the single wavelet transform is the expression of a signal or data set as a linear combination of dilates and translates of a single function. In recent years, this idea has been extended to the so-called multiwavelet case [1–10], in which the signal is expressed as a linear combination of dilates and translates of several functions. Since

[1] Present address with the Division of Engineering and Applied Sciences, Harvard University, Cambridge, MA. E-mail: jkzhang@deas.harvard.edu.

1063-5203/01 $35.00

there are several functions, there is more freedom in the design of multiwavelets than scalar wavelets, and as a result, multiwavelets can simultaneously possess many desired properties such as short support, orthogonality, symmetry, and vanishing moments, which a single wavelet cannot possess simultaneously. This suggests that multiwavelet systems can provide perfect reconstruction, good performance at the boundaries (symmetry), and high approximation order (vanishing moments). Although they look more attractive in theory than scalar wavelets, multiwavelets have yet to realize their advantages in practical applications. One reason for this might be due to the difficulties involved in their proper discrete implementation [11, 12]. The implementation of a multiwavelet transform differs from that of a scalar wavelet transform in that the filter bank requires several input streams. That is, a discrete multiwavelet transform employs a multiple-input, multiple-output (MIMO) filterbank. To generate the multiple streams, some kind of prefiltering of the signal must be performed before the implementation of the multifilter bank [11–14]. However, there are often many ways to do such prefiltering, and different prefilters may lead to different performances [11–14]. In other words, the analysis of a signal based on the multiwavelet transform depends not only on the signal and the multifilter bank, but also on the prefilter. This inconvenices the user and blurs the foreground of multiwavelet applications. It would be far more convenient if the multiwavelet system could be designed so that the projection coefficients for a given scale were the uniform samples of the signal without prefiltering, that is, if a "multiwavelet sampling theorem" were to hold. Scalar systems admitting such a theorem are known to exist [15–20]. Unfortunately, the Haar system is the only two-band orthogonal compactly supported system that possesses this property. (High approximation order M-band systems are available [18–20].) In an attempt to obtain two-band interpolatory multiwavelet systems with high approximation order, Lebrun and Vetterli designed "balanced" multiwavelets [5, 6], but these systems are only quasi-interpolatory [13]. More recently, Selesnick [21] characterized interpolating orthogonal two-band multifilter banks of multiplicity two, and constructed corresponding orthogonal multiwavelet systems that are continuously differentiable.

In this paper we extend Selesnick's analysis to characterize all totally interpolating biorthogonal finite impulse response (FIR) two-band multiplicity-two multifilter bank systems. We then provide a design framework for corresponding compactly supported multiwavelet systems with high approximation order. These systems are "totally interpolating" in the sense that each component of the analysis and synthesis portions possesses the interpolatory property. (In some "interpolatory" scalar schemes [22, 23] only the scaling function is interpolatory.) In addition, we show that for our totally interpolating schemes, the projection of a signal onto a multiwavelet space at a given scale is simply the difference between its projection onto the multiscaling space at the next finer scale and the projection onto the multiscaling space at the given scale. This mimics the structure of the scalar wavelet systems developed by Saito and Beylkin [24] and results in a substantial reduction in the computational cost of implementing the multifilter bank.

This paper is organized as follows. The second section provides an overview of biorthogonal multiwavelet transforms. In the third section, we establish our characterization and design framework, and in the fourth section, we provide examples with approximation order two and three. In the fifth section, we discuss some useful properties of our multiwavelet systems. Finally, we provide a simple but fast decomposition and reconstruction algorithm for our discrete multiwavelet transforms that does not require prefiltering.

2. OVERVIEW OF BIORTHOGONAL MULTIWAVELET TRANSFORM

In this section, we briefly review the fundamental framework of the biorthogonal multiwavelet transform that has been developed recently, e.g., [7, 10]. Let $\boldsymbol{\phi}(t), \tilde{\boldsymbol{\phi}}(t) \in \mathbb{R}^r$ be L^2-stable [2] vector functions in which each element $\phi_i(t), \tilde{\phi}_i(t)$ has compact support, and assume that they satisfy the matrix scaling equations,

$$\boldsymbol{\phi}(t) = 2\sum_k \mathbf{H}_k \boldsymbol{\phi}(2t-k), \tag{2.1}$$

$$\tilde{\boldsymbol{\phi}}(t) = 2\sum_k \tilde{\mathbf{H}}_k \tilde{\boldsymbol{\phi}}(2t-k), \tag{2.2}$$

where $\mathbf{H}_k$ and $\tilde{\mathbf{H}}_k$ denote $r \times r$ matrices. We say that $\boldsymbol{\phi}(t)$ and $\boldsymbol{\phi}(t)$ form a pair of dual (or biorthogonal) multiscaling functions of multiplicity r if they satisfy the condition

$$\langle \boldsymbol{\phi}(t), \tilde{\boldsymbol{\phi}}(t-k)\rangle = \delta(k)\mathbf{I}_r, \qquad \text{for all } k \in \mathbb{Z}, \tag{2.3}$$

where $\delta(k)$ denotes the Kronecker sequence, $\mathbf{I}_r$ denotes the $r \times r$ identity matrix, and $\langle \mathbf{f}, \mathbf{g}\rangle := \int_{-\infty}^{+\infty} \mathbf{f}(t)\mathbf{g}^{\mathrm{T}}(t)\,dt$, where $f(t)$ and $g(t)$ are real. Given $\boldsymbol{\phi}(t)$ and $\tilde{\boldsymbol{\phi}}(t)$, a pair of dual multiwavelet functions of multiplicity r is defined as

$$\boldsymbol{\psi}(t) = 2\sum_{k\in\mathbb{Z}} \mathbf{G}_k \boldsymbol{\phi}(2t-k), \tag{2.4}$$

$$\tilde{\boldsymbol{\psi}}(t) = 2\sum_{k\in\mathbb{Z}} \tilde{\mathbf{G}}_k \tilde{\boldsymbol{\phi}}(2t-k), \tag{2.5}$$

where $\mathbf{G}_k, \tilde{\mathbf{G}}_k \in \mathbb{R}^r$. We say that the analysis system $\{\boldsymbol{\phi}(t), \boldsymbol{\psi}(t)\}$ is a dual of the synthesis system $\{\tilde{\boldsymbol{\phi}}(t), \tilde{\boldsymbol{\psi}}(t)\}$ if it satisfies condition (2.3) and

$$\langle \boldsymbol{\psi}(t), \tilde{\boldsymbol{\psi}}(t-k)\rangle = \delta(k)\mathbf{I}_r, \tag{2.6}$$

$$\langle \boldsymbol{\phi}(t), \tilde{\boldsymbol{\psi}}(t-k)\rangle = \langle \tilde{\boldsymbol{\phi}}(t), \boldsymbol{\psi}(t-k)\rangle = \mathbf{0}, \tag{2.7}$$

for all $k \in \mathbb{Z}$. In order to achieve these, we must have

$$\begin{bmatrix} \mathbf{H}(\omega) & \mathbf{H}(\omega+\pi) \\ \mathbf{G}(\omega) & \mathbf{G}(\omega+\pi) \end{bmatrix} \begin{bmatrix} \tilde{\mathbf{H}}^\dagger(\omega) & \tilde{\mathbf{G}}^\dagger(\omega) \\ \tilde{\mathbf{H}}^\dagger(\omega+\pi) & \tilde{\mathbf{G}}^\dagger(\omega+\pi) \end{bmatrix} = \mathbf{I}_{2r}, \tag{2.8}$$

where $\mathbf{F}(\omega) = \sum_k \mathbf{F}_k e^{-j\omega k}$ and "†" stands for the complex conjugate transpose. This shows that we can attempt to design multiwavelet systems by designing a multifilter bank satisfying the biorthogonal condition (2.8). The procedure is similar to the case of the scalar wavelets. The main difference here lies in the fact that in the vector case, the biorthogonal condition takes a matrix form, and as a result there is more design freedom.

Practical applications usually require that the multiwavelet system possesses several features such as vanishing moments and smoothness, which are closely related to the approximation order of the multiscaling function. A vector function $\boldsymbol{\phi}(t)$ is said to have

[2] A vector function $\boldsymbol{\phi}(t)$ is said to be L^2-*stable* if there exist positive constants A and B such that $A\sum_{k=-\infty}^{\infty} \mathbf{c}_k^H \mathbf{c}_k \le \|\sum_{k=-\infty}^{+\infty} \mathbf{c}_k^H \phi(t-k)\|^2 \le B\sum_{k=-\infty}^{\infty} \mathbf{c}_k^H \mathbf{c}_k$, for any vector sequence $\mathbf{c}_k \in \ell^2$ [7].

approximation order N if there exist vector sequences $\mathbf{y}_k^{(n)}$, $n = 0, 1, \ldots, N-1$, such that

$$\sum_{k\in\mathbb{Z}} (\mathbf{y}_k^{(n)})^{\mathrm{T}} \phi(t-k) = t^n, \qquad \text{for all } t \in \mathbb{R};\ n = 0, \ldots, N-1. \tag{2.9}$$

Similar to the scalar case, the problem of checking whether the vector scaling function has approximation order N can be reduced to the problem of checking whether the corresponding matrix low-pass filter satisfies an Nth-order regularity condition, as shown in the following lemma [4, 7, 9].

LEMMA 1. *Let* $\boldsymbol{\phi}(t)$ *be a compactly supported,* L^2*-stable multiscaling function defined by* (2.1). *Then* $\boldsymbol{\phi}(t)$ *has approximation order* N *if and only if there exist vectors* $\mathbf{y}_0^{(n)} \in \mathbb{R}^r$, $n = 0, 1, \ldots, N-1$, *such that*

$$\sum_{k=0}^{n} \binom{n}{k} (\mathbf{y}_0^{(n)})^{\mathrm{T}} (2j)^{k-n} \mathbf{H}^{(n-k)}(0) = 2^{-n} (\mathbf{y}_0^{(n)})^{\mathrm{T}}, \tag{2.10}$$

$$\sum_{k=0}^{n} \binom{n}{k} (\mathbf{y}_0^{(n)})^{\mathrm{T}} (2j)^{k-n} \mathbf{H}^{(n-k)}(\pi) = \mathbf{0}^{\mathrm{T}}, \tag{2.11}$$

where $\mathbf{0}$ *denotes the zero vector, and* $\mathbf{H}^{(n)}(\omega)$ *denotes the* n*th-order derivative* $\mathbf{H}(\omega)$.

3. TOTALLY INTERPOLATING BIORTHOGONAL MULTIWAVELET SYSTEM

In this section, we build a framework for totally interpolating biorthogonal multiwavelet systems with compact support and design high-approximation-order systems possessing these properties.

A vector function $\mathbf{f}(t) = [f_1(t), f_2(t), \ldots, f_r(t)]^{\mathrm{T}}$ is said to be an *interpolating multifunction* if $\mathbf{f}(t)$ satisfies the condition,

$$\left[\mathbf{f}(n), \mathbf{f}\left(n+\frac{1}{r}\right), \ldots, \mathbf{f}\left(n+\frac{r-1}{r}\right)\right] = \sqrt{r}\,\delta(n)\mathbf{I}_r. \tag{3.1}$$

If each multiscaling function and each multiwavelet function in a biorthogonal multiwavelet system has the interpolating property, we say that the system is *totally interpolating*. In this paper we restrict our focus to the case of $r = 2$. Using (2.1), (2.2), (2.4), and (2.5) we can show that a necessary condition for the biorthogonal multiwavelet system to be a totally interpolating system is that

$$\mathbf{H}(\omega)\begin{bmatrix} 1 & e^{-j\omega} \\ 0 & 0 \end{bmatrix} + \mathbf{H}(\omega+\pi)\begin{bmatrix} 1 & -e^{-j\omega} \\ 0 & 0 \end{bmatrix} = \mathbf{I}_2,$$

and that analogous conditions hold for $\tilde{\mathbf{H}}(\omega)$, $\mathbf{G}(\omega)$, and $\tilde{\mathbf{G}}(\omega)$. These conditions are equivalent to

$$\mathbf{H}(\omega) = \begin{bmatrix} \frac{1}{2} & h_1(\omega) \\ \frac{e^{-j\omega}}{2} & h_2(\omega) \end{bmatrix}, \qquad \tilde{\mathbf{H}}(\omega) = \begin{bmatrix} \frac{1}{2} & \tilde{h}_1(\omega) \\ \frac{e^{-j\omega}}{2} & \tilde{h}_2(\omega) \end{bmatrix}, \tag{3.2}$$

$$\mathbf{G}(\omega) = \begin{bmatrix} \frac{1}{2} & g_1(\omega) \\ \frac{e^{-j\omega}}{2} & g_2(\omega) \end{bmatrix}, \qquad \tilde{\mathbf{G}}(\omega) = \begin{bmatrix} \frac{1}{2} & \tilde{g}_1(\omega) \\ \frac{e^{-j\omega}}{2} & \tilde{g}_2(\omega) \end{bmatrix}, \tag{3.3}$$

where $h_i(\omega)$, $\tilde{h}_i(\omega)$, $g_i(\omega)$, and $\tilde{g}_i(\omega)$ are the frequency responses of scalar filters. (Similar structures have been derived in the orthogonal case [21, 25].) A further necessary condition for the existence of the interpolating $\boldsymbol{\phi}(t)$ and $\tilde{\boldsymbol{\phi}}(t)$ in (2.1) and (2.2) is

$$h_1(0) = h_2(0) = \tilde{h}_1(0) = \tilde{h}_2(0) = \frac{1}{2}.$$

The following theorem, which is proved in Appendix A, shows that the design of a totally interpolating biorthogonal multifilter bank of multiplicity two is equivalent to the design of a corresponding biorthogonal scalar filterbank, in which the analysis filter bank is $\{h_1(\omega), h_2(\omega)\}$ and the synthesis filter bank is $\{\tilde{h}_1(\omega), \tilde{h}_2(\omega)\}$. As such, it extends Selesnick's characterization [21] of interpolating orthogonal multifilter banks of multiplicity two to the biorthogonal case.

THEOREM 1. *Let* $\mathbf{H}(\omega)$ *and* $\tilde{\mathbf{H}}(\omega)$ *be determined by* (3.2). *Then they correspond to the dual matrix low-pass filters in a biorthogonal multifilter bank if and only if*

$$h_1(\omega)\tilde{h}_1(-\omega) + h_1(\pi+\omega)\tilde{h}_1(\pi-\omega) = \frac{1}{2}, \tag{3.4}$$

$$h_2(\omega)\tilde{h}_2(-\omega) + h_2(\pi+\omega)\tilde{h}_2(\pi-\omega) = \frac{1}{2}, \tag{3.5}$$

$$h_1(\omega)\tilde{h}_2(-\omega) + h_1(\pi+\omega)\tilde{h}_2(\pi-\omega) = 0, \tag{3.6}$$

$$h_2(\omega)\tilde{h}_1(-\omega) + h_2(\pi+\omega)\tilde{h}_1(\pi-\omega) = 0. \tag{3.7}$$

Furthermore, if both $h_1(\omega)$ *and* $h_2(\omega)$ *are* FIR (*and hence* $\mathbf{H}(\omega)$ *is* FIR), *then* $\tilde{\mathbf{H}}(\omega)$ *is* FIR *if and only if*

$$h_1(\omega)h_2(\pi+\omega) - h_1(\pi+\omega)h_2(\omega) = ce^{jm\omega} \tag{3.8}$$

for some constant $c \neq 0$ *and some integer* m. *If we take* $c = -\frac{1}{2}$, $m = -1$, *then the corresponding dual matrix low-pass filter is*

$$\tilde{\mathbf{H}}(\omega) = \begin{bmatrix} \frac{1}{2} & -h_2(\pi-\omega)e^{-j\omega} \\ \frac{e^{-j\omega}}{2} & h_1(\pi-\omega)e^{-j\omega} \end{bmatrix}, \tag{3.9}$$

while the matrix high-pass analysis and synthesis filters are given by

$$\mathbf{G}(\omega) = \begin{bmatrix} \frac{1}{2} & -h_1(\omega) \\ \frac{e^{-j\omega}}{2} & -h_2(\omega) \end{bmatrix}, \qquad \tilde{\mathbf{G}}(\omega) = \begin{bmatrix} \frac{1}{2} & h_2(\pi-\omega)e^{-j\omega} \\ \frac{e^{-j\omega}}{2} & -h_1(\pi-\omega)e^{-j\omega} \end{bmatrix}. \tag{3.10}$$

It is well known that symmetry of filterbanks and wavelets plays an important role in some applications (e.g., image processing), and that the generalized interpolating biorthogonal scalar wavelets are symmetric. We would naturally like to obtain symmetric interpolating multifilter banks. A matrix low-pass filter $\mathbf{H}(\omega)$ is said to be symmetric if it satisfies the relationship [9]

$$\mathbf{H}(\omega)\,\mathrm{diag}(\pm e^{-j2T_0}, \ldots, \pm e^{-2jT_{r-1}}) = \mathrm{diag}(\pm e^{-j4T_0}, \ldots, \pm e^{-4jT_{r-1}})\mathbf{H}(-\omega), \tag{3.11}$$

for all $\omega \in \mathbb{R}$ and some constants $T_0, T_1, \ldots, T_{r-1}$. Unfortunately, there are no symmetric totally interpolating biorthogonal multifilter banks with $r = 2$, as we show in the next theorem.

THEOREM 2. *There are no symmetric totally interpolating biorthogonal multifilter banks with* $r = 2$.

The proof of Theorem 2 is given in Appendix B. (In concurrent independent work, Zhou [26] proved a similar result in the orthogonal case.) Theorem 2 tells us that in the two-band case, we cannot design any biorthogonal two-wavelet systems that posses the totally interpolating property and symmetry simultaneously. In the following we will concentrate on designing high-approximation-order totally interpolating biorthogonal multifilter banks and multiwavelet systems with compact support. Theorem 3 provides a design framework for such systems. For notational simplicity, we will choose $c = -\frac{1}{2}$ and $m = -1$ in (3.8).

THEOREM 3. *Let* $\boldsymbol{\phi}(t)$ *and* $\tilde{\boldsymbol{\phi}}(t)$ *be both* L^2*-stable and a pair of dual multiscaling functions defined by* (2.1) *and* (2.2), *respectively, and let the polyphase representations of* $h_i(\omega)$ *in* (3.2) *be*

$$h_i(\omega) = h_{i\mathrm{e}}(2\omega) + e^{-j\omega} h_{i\mathrm{o}}(2\omega) \qquad \text{for } i = 1, 2, \tag{3.12}$$

with $h_{i\mathrm{e}}(\omega)$ *and* $h_{i\mathrm{o}}(\omega)$ *satisfying the condition,*

$$h_{1\mathrm{e}}(\omega) h_{2\mathrm{o}}(\omega) - h_{1\mathrm{o}}(\omega) h_{2\mathrm{e}}(\omega) = \frac{1}{4}. \tag{3.13}$$

Then both $\boldsymbol{\phi}(t)$ *and* $\tilde{\boldsymbol{\phi}}(t)$ *have* N*th-order approximation if and only if*

$$\begin{cases} h_{1\mathrm{e}}^{(n)}(0) = \frac{1+(-1)^n}{2^{2(n+1)}} j^n \\ h_{1\mathrm{o}}^{(n)}(0) = \frac{3^n - 1}{2^{2(n+1)}} j^n \end{cases}, \tag{3.14}$$

and

$$\begin{cases} h_{2\mathrm{e}}^{(n)}(0) = \frac{1-3^n}{2^{2(n+1)}} (-j)^n \\ h_{2\mathrm{o}}^{(n)}(0) = \frac{1+(-1)^n}{2^{2(n+1)}} j^n \end{cases}, \tag{3.15}$$

for $n = 0, 1, \ldots, N-1$, *where notation* $f^{(n)}(0)$ *denotes the nth-order derivative of* $f(\omega)$ *at* $\omega = 0$.

The proof of Theorem 3 is postponed to Appendix C. By Theorem 3, we can transform the construction of high-approximation-order totally interpolating multiwavelet systems with compact support into the construction of a corresponding scalar FIR filter bank satisfying the constraints (3.13)–(3.15). What is different here is that the constraint that the low-pass filters have multiplicity-N zeros at $\omega = \pi$ in the scalar case is now replaced by the constraints (3.14) and (3.15). The design of $h_i(\omega)$ can be accomplished by exploiting an existing design method for scalar biorthogonal filter banks [27]. For instance, given $h_1(z)$, the Z-transform of the filter h_1, solutions to (3.13) exist if and only if $h_{1\mathrm{e}}(z)$ and $h_{1\mathrm{o}}(z)$ are coprime. In that case, $h_2(z)$ can be found by solving the linear equations generated by (3.13) and (3.15).

4. DESIGN EXAMPLES

In this section we will provide two examples of totally interpolating multiwavelet systems with compact support that have approximation order 2 and 3, respectively. In the design, we constrain $h_1(\omega)$ to have the form

$$h_1(\omega) = \sum_{k=-N+1}^{N-1} h_{1,k} e^{-jk\omega}.$$

This shows that we want to design $h_1(\omega)$ of the shortest length such that it satisfies the approximation condition (3.14). Once $h_1(\omega)$ has been determined, by Theorem 3 we can determine the $h_2(\omega)$ of the shortest length such that it satisfies the Nth-order approximation condition (3.15) by checking whether the polyphases $h_{1\mathrm{e}}(\omega)$ and $h_{1\mathrm{o}}(\omega)$ of $h_1(\omega)$ are coprime.

EXAMPLE 1. $N = 2$. In this case, $h_1(\omega)$ takes the form

$$h_1(\omega) = h_{1,-1}e^{j\omega} + h_{1,0} + h_{1,1}e^{-j\omega}.$$

Since $h_1(\omega)$ must satisfy (3.14), we have that

$$h_1(\omega) = \frac{1}{8}e^{j\omega} + \frac{1}{2} - \frac{1}{8}e^{-j\omega}.$$

Correspondingly, $h_{1\mathrm{e}}(\omega) = \frac{1}{2}$ and $h_{1\mathrm{o}}(\omega) = \frac{1}{8}e^{j\omega} - \frac{1}{8}$. It is easily verified that in the $\mathcal{Z}$-domain, $h_{1\mathrm{e}}(z)$ and $h_{1\mathrm{o}}(z)$ have no common root. Hence, by Theorem 3 we can determine $h_2(\omega)$ as

$$h_2(\omega) = \frac{1}{32}e^{j\omega} + \frac{1}{8} + \frac{7}{16}e^{-j\omega} - \frac{1}{8}e^{-2j\omega} + \frac{1}{32}e^{-3j\omega}.$$

By Theorem 1, we obtain

$$\begin{aligned}
\tilde{h}_1\omega &= \frac{1}{32}e^{2j\omega} + \frac{1}{8}e^{j\omega} + \frac{7}{16} - \frac{1}{8}e^{-j\omega} + \frac{1}{32}e^{-2j\omega},\\
\tilde{h}_2(\omega) &= \frac{1}{8} + \frac{1}{2}e^{-j\omega} - \frac{1}{8}e^{-2j\omega},\\
g_1(\omega) &= -\frac{1}{8}e^{j\omega} + \frac{1}{2} - \frac{1}{8}e^{-j\omega},\\
g_2(\omega) &= -\frac{1}{32}e^{2j\omega} - \frac{1}{8} + \frac{7}{16}e^{-j\omega} + \frac{1}{8}e^{-2j\omega} - \frac{1}{32}e^{-3j\omega},\\
\tilde{g}_1(\omega) &= -\frac{1}{32}e^{2j\omega} - \frac{1}{8}e^{j\omega} + \frac{1}{16} + \frac{1}{8}e^{-j\omega} - \frac{1}{32}e^{-2j\omega},\\
\tilde{g}_2(\omega) &= -\frac{1}{8} - \frac{1}{2}e^{-j\omega} + \frac{1}{8}e^{-2j\omega}.
\end{aligned}$$

Using these filters and the corresponding equations (2.1), (2.2), (2.4), and (2.5), it is verified that the constructed multiscaling functions and multiwavelet functions are compactly supported and possess the interpolating property, as shown in Fig. 1 and Fig. 2, respectively. The Sobolev exponents [28] of the analysis multiscaling functions and synthesis

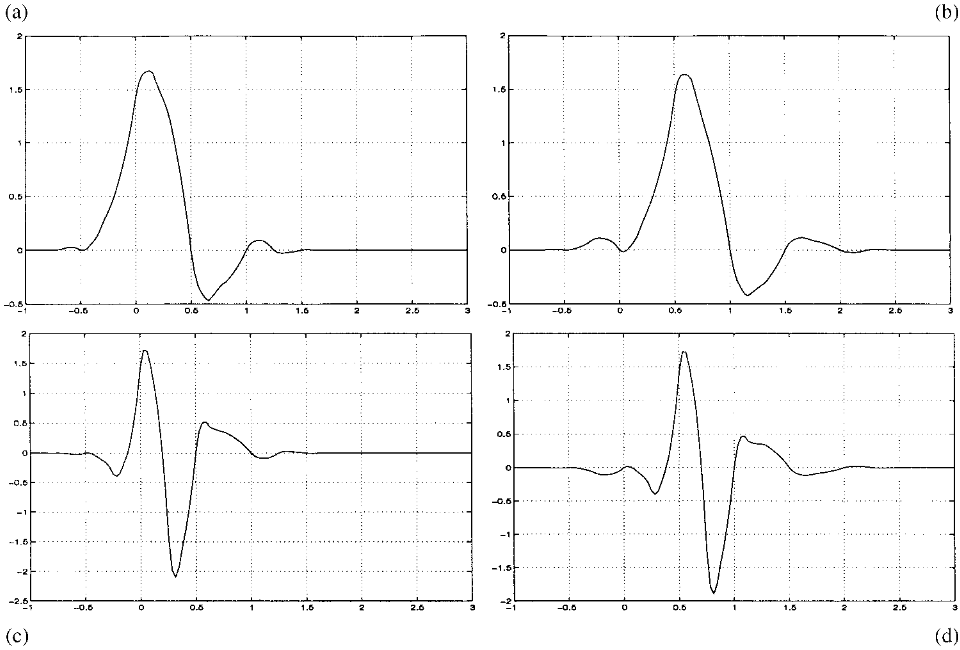

FIG. 1. Second-order analysis interpolating system: (a) multiscaling function $\phi_1(t)$, (b) multiscaling function $\phi_2(t)$, (c) multiwavelet $\psi_1(t)$, (d) multiwavelet function $\psi_2(t)$.

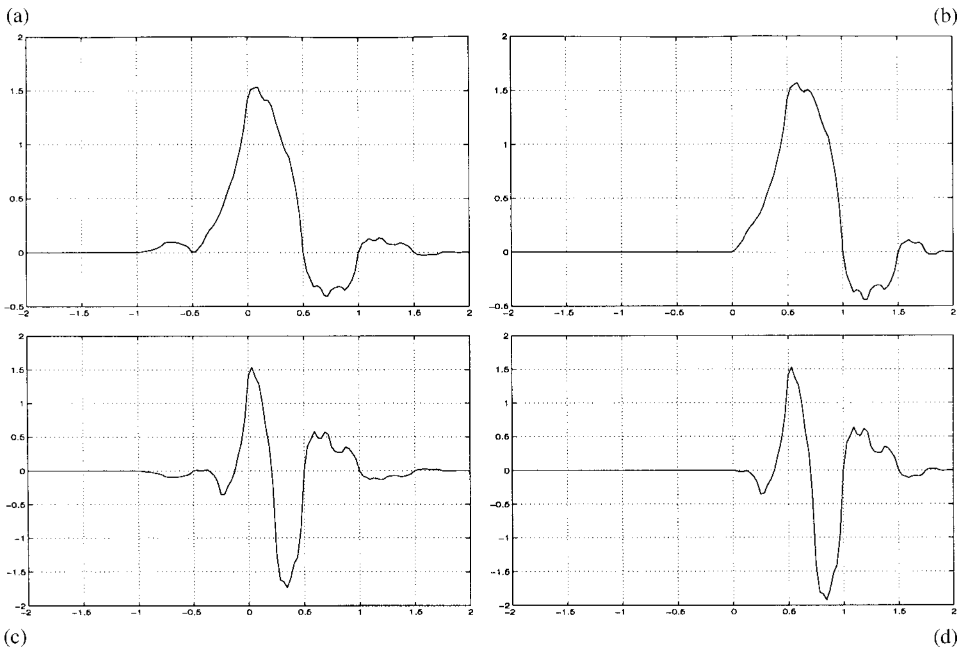

FIG. 2. Second-order synthesis interpolating system: (a) multiscaling function $\tilde{\phi}_1(t)$, (b) multiscaling function $\tilde{\phi}_2(t)$, (c) multiwavelet function $\tilde{\psi}_1(t)$, (d) multiwavelet function $\tilde{\psi}_2(t)$.

multiscaling functions are not less than 1.6237 and 1.2602, respectively.[3] Therefore, the analysis multiscaling functions are continuous and differentiable. Observe that the interpolatory conditions appear to make the multiscaling functions and multiwavelets quite similar in shape. This observation was also made by Selesnick [21] in the orthogonal case.

EXAMPLE 2. $N = 3$. In this case, we let

$$h_1(\omega) = h_{1,-2}e^{2j\omega} + h_{1,-1}e^{j\omega} + h_{1,0} + h_{1,1}e^{-j\omega} + h_{1,2}e^{-2j\omega}.$$

Similar to the procedure of Example 1, after constraining $h_1(\omega)$ so that it satisfies the third-order approximation condition (3.14), we obtain

$$h_1(\omega) = \frac{1}{64}e^{2j\omega} + \frac{1}{8}e^{j\omega} + \frac{15}{32} - \frac{1}{8}e^{-j\omega} + \frac{1}{64}e^{-2j\omega}.$$

By Theorem 1, we have

$$\begin{aligned}
h_2(\omega) &= \frac{1}{512}e^{2j\omega} + \frac{1}{64}e^{j\omega} + \frac{61}{512} + \frac{15}{32}e^{-j\omega} - \frac{61}{512}e^{-2j\omega} + \frac{1}{64}e^{-3j\omega} - \frac{1}{512}e^{-4j\omega},\\
\tilde{h}_1(\omega) &= \frac{1}{512}e^{3j\omega} + \frac{1}{64}e^{2j\omega} + \frac{61}{512}e^{j\omega} + \frac{15}{32} - \frac{61}{512}e^{-j\omega} + \frac{1}{64}e^{-2j\omega} - \frac{1}{512}e^{-3j\omega},\\
\tilde{h}_2(\omega) &= \frac{1}{64}e^{j\omega} + \frac{1}{8} + \frac{15}{32}e^{-j\omega} - \frac{1}{8}e^{-2j\omega} + \frac{1}{64}e^{-3j\omega},\\
g_1(\omega) &= -\frac{1}{64}e^{2j\omega} - \frac{1}{8}e^{j\omega} - \frac{15}{32} + \frac{1}{8}e^{-j\omega} + \frac{1}{64}e^{-2j\omega},\\
g_2(\omega) &= -\frac{1}{128}e^{2j\omega} - \frac{1}{64}e^{j\omega} - \frac{61}{128} - \frac{15}{32}e^{-j\omega} + \frac{61}{128}e^{-2j\omega} - \frac{1}{64}e^{-3j\omega} + \frac{1}{128}e^{-4j\omega},\\
\tilde{g}_1(\omega) &= -\frac{1}{512}e^{3j\omega} - \frac{1}{64}e^{2j\omega} - \frac{61}{512}e^{j\omega} - \frac{1}{15} + \frac{61}{512} - \frac{1}{64}e^{-2j\omega} + \frac{1}{512}e^{-3j\omega},\\
\tilde{g}_2(\omega) &= -\frac{1}{64}e^{j\omega} - \frac{1}{8} - \frac{15}{32}e^{-j\omega} + \frac{1}{8}e^{-2j\omega} - \frac{1}{64}e^{-3j\omega}.
\end{aligned}$$

The multiscaling functions and multiwavelets generated by the above filters all have compact support and possess the interpolating property, as shown in Fig. 3 and Fig. 4, respectively. The Sobolev exponents of analysis multiscaling functions and synthesis multiscaling functions were found to be no less than 1.5 and 1.4801, respectively. A comparison of the order two case with that of order three shows that in the order three case the interpolatory constraint results in greater similarity between the functions. Interestingly, these interpolating multiscaling functions and multiwavelets in Figs. 3 and 4 look so similar that they are almost indistinguishable. In addition, the analysis multiscaling functions do not appear to be any smoother than the order two analysis interpolating multiscaling functions. A similar phenomenon occurs for the orthogonal multiscaling functions presented in [5, 6, 21]; as the balance order increases, the two scaling functions resemble each other more. A possible explanation for this may be that the interpolating condition tends to make the generated multiscaling functions resemble a portion of "sinc" function around its main lobe as the approximation order increases.

[3] These lower bounds were computed using the spectral radius of a restricted transition operator [28].

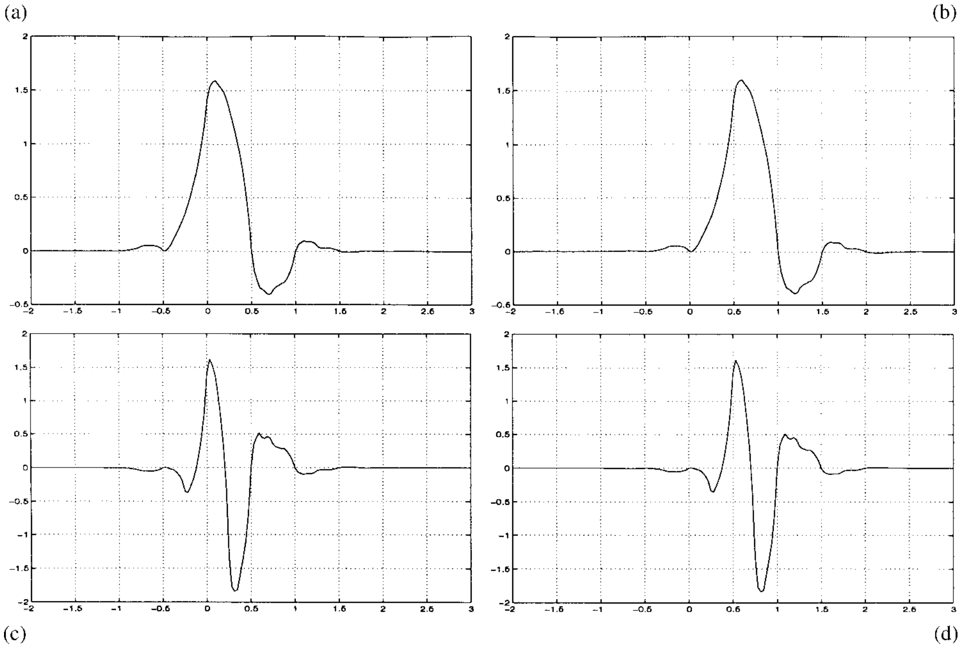

FIG. 3. Third-order analysis interpolating system: (a) multiscaling function $\phi_1(t)$, (b) multiscaling function $\phi_2(t)$, (c) multiwavelet function $\psi_1(t)$ (d) multiwavelet function $\psi_2(t)$.

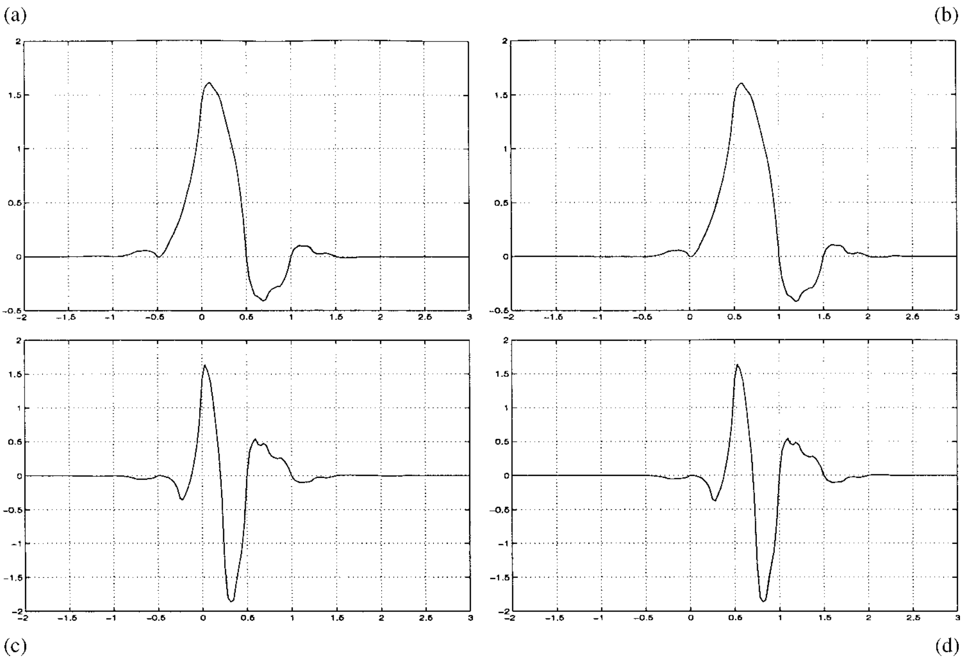

FIG. 4. Third-order synthesis interpolating system: (a) multiscaling function $\tilde{\phi}_1(t)$, (b) multiscaling function $\tilde{\phi}_2(t)$, (c) multiwavelet function $\tilde{\psi}_1(t)$, (d) multiwavelet function $\tilde{\psi}_2(t)$.

5. PROPERTIES OF INTERPOLATING MULTIWAVELETS

In this section, we discuss some important properties of the totally interpolating multiwavelet systems characterized in Theorems 1 and 3.

PROPERTY 1. *For $n = 0, 1, 2, \ldots, N-1$, we have*

$$\hat{\boldsymbol{\phi}}^{(n)}(0) = \left[\delta(n), \left(-\frac{j}{2}\right)^n\right]^{\mathrm{T}}, \tag{5.1}$$

$$\hat{\tilde{\boldsymbol{\phi}}}^{(n)}(0) = \left[\delta(n), \left(-\frac{j}{2}\right)^n\right]^{\mathrm{T}}, \tag{5.2}$$

$$\hat{\boldsymbol{\psi}}^{(n)}(0) = \mathbf{0}, \tag{5.3}$$

$$\hat{\tilde{\boldsymbol{\psi}}}^{(n)}(0) = \mathbf{0}, \tag{5.4}$$

where $\hat{f}(\omega)$ denotes the Fourier transform of $f(t)$ and $\hat{f}^{(n)}(\omega)$ denotes the nth-order derivative of $\hat{f}(\omega)$.

Property 1 shows that the functions $\hat{\phi}_1(\omega)$, $e^{j\omega/2}\hat{\phi}_2(\omega)$, $\hat{\tilde{\phi}}_1(\omega)$, and $e^{j\omega/2}\hat{\tilde{\phi}}_2(\omega)$ have Nth-order flatness near zero frequency and that the multiwavelet functions $\psi(t)$ and $\tilde{\psi}(t)$ have Nth-order vanishing moments; i.e.,

$$\int_{-\infty}^{+\infty} t^n \psi(t)\, dt = \int_{-\infty}^{+\infty} t^n \tilde{\psi}(t)\, dt = 0, \qquad \text{for } n = 0, 1, \ldots, N-1. \tag{5.5}$$

Proof of Property 1. Since $\tilde{\boldsymbol{\phi}}(t)$ has approximation order N, (2.12) holds with respect to $\tilde{\boldsymbol{\phi}}(t)$ for $n = 0, 1, \ldots, N-1$; i.e.,

$$\sum_{k\in\mathbb{Z}} (\tilde{\mathbf{y}}_k^{(n)})^{\mathrm{T}} \tilde{\boldsymbol{\phi}}(t-k) = t^n, \qquad t \in \mathbb{R}. \tag{5.6}$$

In addition, since $\tilde{\boldsymbol{\phi}}(t)$ possesses the interpolating property, setting $t = 0$ and $t = \frac{1}{2}$ in (5.6), respectively, we obtain

$$\tilde{\mathbf{y}}_0^{(n)} = \frac{1}{\sqrt{2}}[\delta(n), 2^{-n}]^{\mathrm{T}}, \qquad \text{for } n = 0, 1, \ldots, N-1. \tag{5.7}$$

Noting that

$$\hat{\boldsymbol{\phi}}^{(n)}(0) = (-j)^n \int_{-\infty}^{+\infty} t^n \boldsymbol{\phi}(t)\, dt, \tag{5.8}$$

$$\hat{\boldsymbol{\psi}}^{(n)}(0) = (-j)^n \int_{-\infty}^{+\infty} t^n \boldsymbol{\psi}(t)\, dt, \tag{5.9}$$

and by substituting (5.6) into (5.8) and (5.9), respectively, we have

$$\begin{aligned}\hat{\boldsymbol{\phi}}^{(n)}(0) &= (-j)^n \sum_{l\in\mathbb{Z}} \left(\int_{-\infty}^{+\infty} \boldsymbol{\phi}(t)\tilde{\boldsymbol{\phi}}^{\mathrm{T}}(r-l)\, dt\right)\mathbf{y}_l^{(n)} \\ &= \sqrt{2}(-j)^n \sum_{l\in\mathbb{Z}} \delta(l)\mathbf{I}_2\mathbf{y}_l^{(n)} = \left[\delta(n), \left(-\frac{j}{2}\right)^n\right]^{\mathrm{T}}\end{aligned} \tag{5.10}$$

$$\hat{\boldsymbol{\psi}}^{(n)}(0) = (-j)^n \sum_{l\in\mathbb{Z}} \left(\int_{-\infty}^{+\infty} \boldsymbol{\psi}(t)\tilde{\boldsymbol{\phi}}^{\mathrm{T}}(t-l)\,dt \right) \mathbf{y}_l^{(n)} = \mathbf{0}. \tag{5.11}$$

Here we have used the biorthogonality conditions in (2.3) and (2.7). Similar techniques lead to (5.2) and (5.4). ■

Similar to the scalar case, the interpolating multiscaling functions and multiwavelets have also the following property described in [29]. The property shows that interpolating multiscaling functions and multiwavelets are uniquely determined by uniform samples of themselves at the points $\{n/4\}_{n\in\mathbb{Z}}$.

PROPERTY 2.

$$\boldsymbol{\phi}(t) = \frac{1}{\sqrt{2}} \sum_m \boldsymbol{\Phi}(m)\boldsymbol{\phi}(2t-m), \qquad \tilde{\boldsymbol{\phi}}(t) = \frac{1}{\sqrt{2}} \sum_m \tilde{\boldsymbol{\Phi}}(m)\tilde{\boldsymbol{\phi}}(2t-m), \tag{5.12}$$

$$\boldsymbol{\psi}(t) = \frac{1}{\sqrt{2}} \sum_m \boldsymbol{\Psi}(m)\boldsymbol{\psi}(2t-m), \qquad \tilde{\boldsymbol{\psi}}(t) = \frac{1}{\sqrt{2}} \sum_m \tilde{\boldsymbol{\Psi}}(m)\tilde{\boldsymbol{\psi}}(2t-m), \tag{5.13}$$

where for any $m \in \mathbb{Z}$,

$$\boldsymbol{\Phi}(m) = \begin{bmatrix} \boldsymbol{\phi}_1(\frac{m}{2}) & \boldsymbol{\phi}_1(\frac{2m+1}{4}) \\ \boldsymbol{\phi}_2(\frac{m}{2}) & \boldsymbol{\phi}_2(\frac{2m+1}{4}) \end{bmatrix}, \qquad \tilde{\boldsymbol{\Phi}}(m) = \begin{bmatrix} \tilde{\boldsymbol{\phi}}_1(\frac{m}{2}) & \tilde{\boldsymbol{\phi}}_1(\frac{2m+1}{4}) \\ \tilde{\boldsymbol{\phi}}_2(\frac{m}{2}) & \tilde{\boldsymbol{\phi}}_2(\frac{2m+1}{4}) \end{bmatrix}, \tag{5.14}$$

$$\boldsymbol{\Psi}(m) = \begin{bmatrix} \boldsymbol{\psi}_1(\frac{m}{2}) & \boldsymbol{\psi}_1(\frac{2m+1}{4}) \\ \boldsymbol{\psi}_2(\frac{m}{2}) & \boldsymbol{\psi}_2(\frac{2m+1}{4}) \end{bmatrix}, \qquad \tilde{\boldsymbol{\Psi}}(m) = \begin{bmatrix} \tilde{\boldsymbol{\psi}}_1(\frac{m}{2}) & \tilde{\boldsymbol{\psi}}_1(\frac{2m+1}{4}) \\ \tilde{\boldsymbol{\psi}}_2(\frac{m}{2}) & \tilde{\boldsymbol{\psi}}_2(\frac{2m+1}{4}) \end{bmatrix}. \tag{5.15}$$

Proof of Property 2. We here select one of the properties, the first equation of (5.12). The proofs of the others are similar. In (2.1), taking $t = m/2$ and $t = (2m+1)/4$, we have

$$\boldsymbol{\phi}\left(\frac{m}{2}\right) = 2\sum_k \mathbf{H}_k \boldsymbol{\phi}(m-k), \tag{5.16}$$

$$\boldsymbol{\phi}\left(\frac{2m+1}{4}\right) = 2\sum_k \mathbf{H}_k \boldsymbol{\phi}\left(m-k+\frac{1}{2}\right). \tag{5.17}$$

The above two equations can be rewritten in a more compact form as

$$\boldsymbol{\Phi}(m) = 2\sum_k \mathbf{H}_k \left[\boldsymbol{\phi}(m-k), \boldsymbol{\phi}\left(m-k+\frac{1}{2}\right) \right]. \tag{5.18}$$

Now applying the interpolating property of $\boldsymbol{\phi}(t)$ to (5.18) yields

$$\boldsymbol{\Phi}(m) = 2\sqrt{2}\sum_k \mathbf{H}_k \delta(m-k)\mathbf{I}_2 = 2\sqrt{2}\mathbf{H}_m, \tag{5.19}$$

from which it follows that $\mathbf{H}_m = (1/2\sqrt{2})\Phi(m)$ for all $m \in \mathbb{Z}$. This completes the proof. ■

For a general biorthogonal multi wavelet system, define

$$V_J\left([\phi_1(t), \phi_2(t)]^{\mathrm{T}}\right) = \mathrm{span}\left\{\phi_1(2^J t - n), \phi_2(2^J t - k)\right\}_{k,n\in\mathbb{Z}}.$$

Similarly, we can define $V_J(\tilde{\boldsymbol{\phi}})$, $V_J(\boldsymbol{\psi})$, and $V_J(\tilde{\boldsymbol{\psi}})$. Then $f(t) \in V_0(\boldsymbol{\phi})$ can be expressed as [11]

$$f(t) = \sum_n \langle f(t), \tilde{\phi}_1(t-n)\rangle \phi_1(t-n) + \sum_k \langle f(t), \tilde{\phi}_2(t-k)\rangle \phi_2(t-k). \tag{5.20}$$

Fortunately, our multiwavelet system is totally interpolating and hence the inner products in (5.20), which can be awkward to compute in practice [11], are equal to uniform samples of $f(t)$, as shown in the following property.

PROPERTY 3.

$$f(t) = \sum_{k\in\mathbb{Z}} f(k)\phi_1(t-k) + \sum_{k\in\mathbb{Z}} f(k+1/2)\phi_2(t-k), \qquad \textit{for all } f(t) \in V_0(\boldsymbol{\phi}),$$

and analogous statements hold for the functions in $V_0(\tilde{\boldsymbol{\phi}})$, $V_0(\boldsymbol{\psi})$, *and* $V_0(\tilde{\boldsymbol{\psi}})$.

Property 3 resembles the classical Shannon Sampling Theorem for bandlimited signals: For all $\sigma\pi$ bandlimited signals, i.e., all $f(t)$ such that $\hat{f}(\omega) \subset (-\sigma\pi, \sigma\pi)$,

$$f(t) = \sum_n f\left(\frac{n}{\sigma}\right) \operatorname{sinc}(\sigma t - n),$$

where $\operatorname{sinc}(x) = \sin(\pi x)/(\pi x)$. That is, $f(t)$ can be reconstructed from uniform samples of itself using translates of a single synthesis function, the sinc function. In contrast, the signals in Property 3 are reconstructed for uniform samples of themselves using translates of two synthesis functions. An advantage of the multiwavelet system is that the choice of the synthesis functions is quite flexible. In the bandlimited case we are constrained to use the sinc function which is not compactly supported and decays very slowly in time. In contrast, the synthesis functions in Property 3 are compactly supported in time. As a result, if a signal $s(t)$ in the multiscaling or multiwavelet subspaces is continuous, then one is able to reconstruct it quickly without errors induced by the truncation of the synthesis function, via a fast recursive algorithm (illustrated below). Moreover, there is a large set of candidate synthesis functions that satisfy Property 3. Although this design freedom can increase complexity of the application of multiwavelets to practical problems, it allows us to tailor the transform to the application at hand. To illustrate the application of Property 3, we consider a continuous signal $s(t)$ in $V_0(\boldsymbol{\phi})$. Using the nested property of multiresolution subsapces we know that if signal $s(t) \in V_0(\boldsymbol{\phi})$, then $s(t) \in V_i(\boldsymbol{\phi})$ for any $i \geq 0$. Therefore, if we have obtained signal samples $\mathbf{s}_i(k) = [s(k/2^i), s((2k+1)/2^{i+1})]^{\mathrm{T}}$, then, applying Property 3 with multiresolution subspace $V_i(\boldsymbol{\phi})$ results in

$$s(t) = \sum_{n\in\mathbb{Z}} s\left(\frac{n}{2^i}\right)\phi_1(2^i t - n) + \sum_{n\in\mathbb{Z}} s\left(\frac{2n+1}{2^{i+1}}\right)\phi_2(2^i t - k). \tag{5.21}$$

Similar to the procedure in the proof of Property 2, setting $t = k/2^{i+1}$, and $t = (2k+1)/2^{i+2}$, respectively, we obtain the matrix form

$$\mathbf{s}_{i+1}(k) = \sum_n \boldsymbol{\Phi}^{\mathrm{T}}(k-2n)\mathbf{s}_i(n), \tag{5.22}$$

where $\mathbf{\Phi}(m)$ is defined by the first equation of (5.14). On the other hand, we know from the proof of Property 2 that $\mathbf{\Phi}(k-2n) = 2\sqrt{2}\mathbf{H}_{k-2n}$. Combining these results yields

$$\mathbf{s}_{i+1}(k) = 2\sqrt{2}\sum_n \mathbf{H}_{k-2n}^{\mathrm{T}}\mathbf{s}_i(n). \tag{5.23}$$

Property 3 also implies that the projection coefficients of a signal at a given scale are exactly consistent with the uniform sampling points of the signal, and hence that the laborious prefiltering procedure that must normally be performed before the implementation of standard discrete multiwavelet transforms can be avoided.

PROPERTY 4.

$$\psi_1(t) = 2\phi_1(2t) - \phi_1(t), \tag{5.24}$$

$$\psi_2(t) = 2\phi_1(2t-1) - \phi_2(t), \tag{5.25}$$

$$\tilde{\psi}_1(t) = 2\tilde{\phi}_1(2t) - \tilde{\phi}_1(t), \tag{5.26}$$

$$\tilde{\psi}_2(t) = 2\tilde{\phi}_1(2t-1) - \tilde{\phi}_2(t). \tag{5.27}$$

Proof. Note that in totally interpolating multiwavelet systems designed by Theorem 3, the analysis scaling equation and the wavelet equation can be expressed, respectively, as

$$\phi_1(t) = \phi_1(2t) + 2\sum_k h_{1,k}\phi_2(2t-k), \tag{5.28}$$

$$\phi_2(t) = \phi_1(2t-1) + 2\sum_k h_{2,k}\phi_2(2t-k), \tag{5.29}$$

$$\psi_1(t) = \phi_1(2t) - 2\sum_k h_{1,k}\phi_2(2t-k), \tag{5.30}$$

$$\psi_2(t) = \phi_1(2t-1) - 2\sum_k h_{2,k}\phi_2(2t-k). \tag{5.31}$$

Combining (5.28) with (5.30) yields (5.24), while combining (5.29) with (5.31) yields (5.25). Similarly, we can obtain (5.26) and (5.27). This completes the proof of Property 4. ■

It can be seen from Property 4 that the designed multiwavelet system has the same structure as that designed by Saito and Beylkin [24] in the scalar case. However, in their designed interpolating biorthogonal scalar wavelet system, only one function possesses the interpolating property and the system is not compactly supported. In our multiwavelet scheme all functions are interpolating and compactly supported. In fact, Property 4 gives a simple, but fast, totally interpolating discrete multiwavelet transform without prefiltering. Let $f(t) \in V_J(\boldsymbol{\phi})$, and let $c_i^{(j)}(k) = 2^{-j/2}\int_{-\infty}^{+\infty} f(t)\tilde{\phi}_i(2^j t - k)\,dt$ and $d_i^{(j)}(k) = 2^{-j/2}\int_{-\infty}^{+\infty} f(t)\tilde{\psi}_i(2^j t - k)\,dt$. Then $c_1^{(J)}(k) = f(k/2^J)$, $c_2^{(J)}(k) = f((2k+1)/2^{J+1})$. In this case, the decomposition algorithm is

$$c_1^{(j-1)}(k) = \frac{\sqrt{2}}{2}c_1^{(j)}(2k) + \sqrt{2}\sum_n h_{1,n}c_2^{(j)}(2k+n),$$

$$c_2^{(j-1)}(k) = \frac{\sqrt{2}}{2}c_1^{(j)}(2k+1) + \sqrt{2}\sum_n h_{2,n}c_2^{(j)}(2k+n),$$

$$d_1^{(j-1)}(k) = \sqrt{2}c_1^{(j)}(2k) - c_2^{(j-1)}(k),$$

$$d_2^{(j-1)}(k) = \sqrt{2}c_1^{(j)}(2k+1) - c_2^{(j-1)}(k),$$

for $j = J, J-1, \ldots$, while the reconstruction algorithm is

$$c_1^{(j)}(2k) = \frac{\sqrt{2}}{2}\left(d_1^{(j-1)}(k) + c_2^{(j-1)}(k)\right),$$

$$c_1^{(j)}(2k+1) = \frac{\sqrt{2}}{2}\left(d_2^{(j-1)}(k) + c_2^{(j-1)}(k)\right),$$

$$\begin{aligned} c_2^{(j)}(n) &= \sqrt{2}\sum_k (-1)^{(k-1)} h_{2,1-k}\left(c_1^{(j-1)}(2k+n) - d_1^{(j-1)}(2k+n)\right) \\ &\quad + \sqrt{2}\sum_k (-1)^k h_{1,1-k}\left(c_2^{(j-1)}(2k+n) - d_2^{(j-1)}(2k+n)\right) \end{aligned}$$

for $j = \ldots, J-1, J$.

6. CONCLUSIONS

In this paper, we proposed a systematic scheme for the design of high-approximation-order totally interpolating biorthogonal FIR filter banks and multiwavelet systems with compact support. An important property of our design is that each component of the analysis system and each component of the synthesis system possess the interpolating property. We transformed the problem of designing a totally interpolating biorthogonal multiwavelet system of multiplicity two into the problem of designing a corresponding biorthogonal scalar wavelet system. Therefore, they are easily designed. We constructed two examples to illustrate some features of the totally interpolating multiwavelet systems. Moreover, we discussed some important properties of this kind of system. In addition to sharing some common advantages of the interpolating scalar wavelet system, such as the dyadic rational nature of the filter coefficients, equality of the flatness degree of the low-pass filters with the approximation order of the scaling function and equality between the uniform samples of a signal and its projection coefficients for a given scale, our multiwavelet systems possess their own characteristics. One is that any continuous signal in a multiresolution subspace can be reconstructed quickly via a simple recursive algorithm without errors induced by truncation of the synthesis function. This suggests that prefiltering is not necessary for the totally interpolating discrete biorthogonal multiwavelet transform. The other is that there is a simple relationship between the multiscaling functions and the multiwavelets. This relationship substantially simplifies the implementation of the system.

APPENDIX

A. *Proof of Theorem 1*

Using (3.2), the (1,1) block of the biorthogonal condition (2.8) is equivalent to

$$\mathbf{A}(\omega)\tilde{\mathbf{A}}^*(\omega) = \frac{1}{2}\mathbf{I}, \tag{A.1}$$

where

$$\mathbf{A}(\omega) = \begin{bmatrix} h_1(\omega) & h_1(\pi+\omega) \\ h_2(\omega) & h_2(\pi+\omega) \end{bmatrix}, \qquad \tilde{\mathbf{A}}(\omega) = \begin{bmatrix} \tilde{h}_1(\omega) & \tilde{h}_1(\pi+\omega) \\ \tilde{h}_2(\omega) & \tilde{h}_2(\pi+\omega) \end{bmatrix}. \tag{A.2}$$

Comparing (A.2) with the standard "modulation domain" condition [30] for a scalar filterbank to have perfect reconstruction, it is clear that $\{h_1, h_2\}$ and $\{\tilde{h}_1, \tilde{h}_2\}$ constitute a biorthogonal scalar filter bank, in which the analysis filter bank is $\{h_1, h_2\}$, while the synthesis filter bank is $\{\tilde{h}_1, \tilde{h}_2\}$. We know from the theory of scalar filter banks [30–32] that if $\{h_1, h_2\}$ is FIR, then $\{\tilde{h}_1, \tilde{h}_2\}$ is FIR if and only if

$$\det \mathbf{A}(\omega) = ce^{jm\omega} \tag{A.3}$$

for some constant $c \neq 0$ and some integer m. Combining (A.1) with (A.4) yields

$$\tilde{\mathbf{A}}(\omega) = \mathbf{A}^{-1}(\omega) = \frac{1}{2c} e^{-jm\omega} \begin{bmatrix} h_2(\pi+\omega) & -h_1(\omega) \\ -h_2(\pi+\omega) & h_1(\pi+\omega) \end{bmatrix}. \tag{A.4}$$

If we take $c = -\frac{1}{2}$ and $m = -1$, it follows from (A.3) and (A.4) that

$$\tilde{h}_1(\omega) = -h_2(\pi-\omega)e^{-j\omega}, \tag{A.5}$$

$$\tilde{h}_2(\omega) = h_1(\pi-\omega)e^{-j\omega}, \tag{A.6}$$

and hence (3.9). Using similar arguments, we can show that (3.3) and the (2,2) block of (2.8) lead to equations analogous to (3.4)–(3.8), but with the h's replaced by g's. What remains to be shown is that $g_1(\omega)$, $g_2(\omega)$, $\tilde{g}_1(\omega)$ and $\tilde{g}_2(\omega)$ have the form shown in (3.10). Using the (1,2) block of (2.8) and the structure of $\mathbf{H}(\omega)$ and $\tilde{\mathbf{G}}(\omega)$ in (3.2) and (3.3) we have that

$$\begin{bmatrix} h_1(-\omega) & h_1(-\omega+\pi) \\ h_2(-\omega) & h_2(-\omega+\pi) \end{bmatrix} \begin{bmatrix} \tilde{g}_1(\omega) \\ \tilde{g}_1(\omega+\pi) \end{bmatrix} = \begin{bmatrix} -\frac{1}{2} \\ 0 \end{bmatrix}, \tag{A.7}$$

$$\begin{bmatrix} h_1(-\omega) & h_1(-\omega+\pi) \\ h_2(-\omega) & h_2(-\omega+\pi) \end{bmatrix} \begin{bmatrix} \tilde{g}_2(\omega) \\ \tilde{g}_2(\omega+\pi) \end{bmatrix} = \begin{bmatrix} 0 \\ -\frac{1}{2} \end{bmatrix}. \tag{A.8}$$

Using (A.3) with $c = -\frac{1}{2}$ and $m = -1$ we obtain $\tilde{g}_1(\omega) = h_2(\pi-\omega)e^{-j\omega}$ and $\tilde{g}_2(\omega) = h_1(\pi-\omega)e^{-j\omega}$. The remaining filters $g_1(\omega)$ and $g_2(\omega)$ can be found from the equivalent equations to (A.5) and (A.6) for the g filters. This completes the proof of Theorem 1. ■

B. Proof of Theorem 2

If such a pair of filters exists, then it must satisfy the symmetrical relationship [9]

$$\mathbf{H}(\omega)\,\mathrm{diag}(\pm e^{-j2T_0}, \pm e^{-2jT_1}) = \mathrm{diag}(\pm e^{-j4T_0}, \pm e^{-j4T_1})\mathbf{H}(-\omega),$$

where T_i are the symmetry points of ϕ_i, the "+" symbol denotes that $\phi_i(t)$ is symmetric about T_i, while the "−" symbol denotes that ϕ_i is antisymmetric about T_i for $i = 1, 2$. Independent of the symmetry, we obtain $h_1(\omega) = h_1(-\omega)e^{j\omega}$, $h_2(\omega) = h_2(-\omega)e^{-j\omega}$, which implies that $h_1(\pi) = h_2(\pi) = 0$. It follows from (3.4)–(3.7) that $h_1(0)\tilde{h}_1(0) = h_2(0)\tilde{h}_2(0) = \frac{1}{2}$ and $h_1(0)\tilde{h}_2(0) = h_2(0)\tilde{h}_1(0) = 0$ hold simultaneously, which leads to a contradiction. This completes the proof of Theorem 2. ■

C. Proof of Theorem 3

We first prove that if both the interpolating multiscaling function $\boldsymbol{\phi}(t)$ and its dual interpolating multiscaling function $\tilde{\boldsymbol{\phi}}(t)$ can provide approximation order N, then

$$\begin{cases} \mathbf{y}_0^{(0)} = \tilde{\mathbf{y}}_0^{(0)} = \frac{1}{\sqrt{2}}[1, 1]^{\mathrm{T}} \\ \mathbf{y}_k^{(n)} = \tilde{\mathbf{y}}_k^{(n)} = \frac{1}{\sqrt{2}}[k^n, (k+\frac{1}{2})^n]^{\mathrm{T}} \end{cases} \tag{C.1}$$

for $n = 1, 2, \ldots, N-1$ and for all $k \in \mathbb{Z}$, $k \neq 0$. In fact, we know that both $\boldsymbol{\phi}(t)$ and $\tilde{\boldsymbol{\phi}}(t)$ have approximation order N if and only if they satisfy (2.12) simultaneously. Equation (C.1) then follows from the interpolating property. Then using Lemma 1 with the interpolating low-pass matrix filters of the form in (3.2), we know that interpolating multiscaling function $\boldsymbol{\phi}(t)$ can provide approximation order N if only and if

$$\begin{cases} \sum_{k=1}^{n} \binom{n}{k} j^k h_2^{(n-k)}(0) + h_1^{(n)}(0) + h_2^{(n)}(0) = (\frac{j}{2})^n, \\ \sum_{k=1}^{n} \binom{n}{k} j^k h_2^{(n-k)}(\pi) + h_1^{(n)}(\pi) + h_2^{(n)}(\pi) = 0, \end{cases} \tag{C.2}$$
$$\text{for } n = 0, 1, \ldots, N-1.$$

Let

$$\begin{cases} a(\omega) = e^{j\omega} h_2(\omega) + h_1(\omega), \\ b(\omega) = -e^{j\omega} h_2(\omega) + h_1(\omega). \end{cases} \tag{C.3}$$

Then (C.2) is equivalent to

$$\begin{cases} a^{(n)}(0) = (\frac{j}{2})^n, \\ b^{(n)}(\pi) = 0, \end{cases} \tag{C.4}$$

for $n = 0, 1, 2, \ldots, N-1$. Using the notation in (3.2) we define

$$u(\omega) = h_{1\mathrm{e}}(2\omega) + e^{j\omega} h_{2\mathrm{e}}(2\omega), \tag{C.5}$$

$$v(\omega) = h_{2\mathrm{o}}(2\omega) + e^{j\omega} h_{1\mathrm{o}}(2\omega), \tag{C.6}$$

and define $\tilde{u}(\omega)$ and $\tilde{v}(\omega)$ in a analogous way. Then (C.3) becomes

$$\begin{cases} a(\omega) = u(\omega) + v(\omega), \\ b(\pi + \omega) = u(\omega) - v(\omega). \end{cases} \tag{C.7}$$

Taking the nth derivative of both sides of (C.7) at $\omega = 0$ and using (C.4) leads to

$$u^{(n)}(0) + v^{(n)}(0) = \frac{j^n}{2^n}, \tag{C.8}$$

$$u^{(n)}(0) - v^{(n)}(0) = 0. \tag{C.9}$$

From these two equations we have that

$$u^{(n)}(0) = \frac{j^n}{2^{n+1}}, \qquad v^{(n)}(0) = \frac{j^n}{2^{n+1}}, \tag{C.10}$$

for $n = 0, 1, 2, \ldots, N-1$. Similarly, we can obtain

$$\tilde{u}^{(n)}(0) = \frac{j^n}{2^{n+1}}, \qquad \tilde{v}^{(n)}(0) = \frac{j^n}{2^{n+1}}, \tag{C.11}$$

for $n = 0, 1, 2, \ldots, N-1$. On the other hand, from (3.9) we have that $\tilde{h}_{1e}(\omega) = h_{2o}(-\omega)$, $\tilde{h}_{1o}(\omega) = -h_{2e}(-\omega)$, $\tilde{h}_{2e}(\omega) = -h_{1o}(-\omega)$, and $\tilde{h}_{2o}(\omega) = h_{1e}(-\omega)$. Therefore,

$$\tilde{u}(\omega) = h_{2o}(-2\omega) - e^{j\omega} h_{1o}(-2\omega), \tag{C.12}$$

$$\tilde{v}(\omega) = h_{1e}(-2\omega) - e^{-j\omega} h_{2e}(-2\omega). \tag{C.13}$$

We obtain from (C.5) and (C.13) that

$$h_{1e}(\omega) = \frac{1}{2}\left(u\left(\frac{\omega}{2}\right) + \tilde{v}\left(-\frac{\omega}{2}\right)\right), \tag{C.14}$$

$$h_{2e}(\omega) = \frac{1}{2}\left(u\left(\frac{\omega}{2}\right) - \tilde{v}\left(-\frac{\omega}{2}\right)\right) e^{-j\omega/2}. \tag{C.15}$$

Similarly, combining (C.6) with (C.12) leads to

$$h_{1o}(\omega) = \frac{1}{2}\left(v\left(\frac{\omega}{2}\right) - \tilde{u}\left(-\frac{\omega}{2}\right)\right) e^{j\omega/2}, \tag{C.16}$$

$$h_{2o}(\omega) = \frac{1}{2}\left(v\left(\frac{\omega}{2}\right) + \tilde{u}\left(-\frac{\omega}{2}\right)\right). \tag{C.17}$$

Finally, taking the nth derivatives of (C.14)–(C.17) at $\omega = 0$, respectively, and utilizing the corresponding results (C.10) and (C.11), we complete the proof of Theorem 3. ■

ACKNOWLEDGMENTS

The first author thanks Professor Bao Zheng for his careful guidance at Xidian University, Xi'an, China. This work is an extension of his Ph.D. dissertation. He also thanks the support of the National Natural Science Foundation of China (Grant 69772029), and the National Sciences and Engineering Research Council of Canada (Grant 4464-00).

REFERENCES

1. T. N. Goodman, S. L. Lee, and W. S. Tang, Wavelets in wandering subspaces, *Trans. Amer. Math. Soc.* **338** (1993), 639–654.
2. J. Geronimo, D. P. Hardin, and P. Massopust, Fractal functions and wavelet expansions based on several scaling functions, *J. Approx. Theory* **78** (1994), 2373–2401.
3. G. Strang and V. Strela, Short wavelets and matrix dilation equations, *IEEE Trans. Signal Process.* **43** (1995), 108–115.
4. W. Lawton, S. L. Lee, and Z. Shen, An algorithm for matrix extension and wavelet construction, *Math. Comput.* **65** (1996), 723–737.
5. J. Lebrun and M. Vetterli, Balanced multiwavelets—Theory and design, *IEEE Trans. Signal Process.* **46** (1998), 1119–1125.
6. J. Lebrun and M. Vetterli, High order balanced multiwavelets, in "Proc. Int. Conf. Acoustics, Speech Signal Processing," pp. 373–386, 1998.
7. G. Plonka and V. Strela, From wavelets to multiwavelets, in "Mathematical Methods for Curves and Surfaces II" (M. Dahlen, T. Lyche, and L. L. Schumaker, Eds.), pp. 375–399, Vanderbilt Univ. Press, Nashville, 1998.
8. Q. Jiang, On the design of multifilter banks and orthogonal multiwavelets, *IEEE Trans. Signal Process.* **46** (1998), 3292–3303.
9. G. Plonka and V. Strela, Construction of multiscaling function's with approximation and symmetry, *SIAM J. Math. Anal.* **29** (1998), 481–510.

10. V. Strela, P. N. Heller, G. Strang, P. Topiwala, and C. Heil, The application of multiwavelet filterbanks to image processing, *IEEE Trans. Image Process.* **6** (1999), 548–563.
11. X.-G. Xia, D. P. Hardin, J. Geronimo, and B. Suter, Design of prefilters for discrete multiwavelet transform, *IEEE Trans. Signal Process.* **44** (1996), 25–35.
12. X.-G. Xia, A new prefilter design for discrete multiwavelet transforms, *IEEE Trans. Signal Process.* **46** (1998), 1558–1570.
13. D. P. Hardin and D. W. Roach, Multiwavelet prefilters I: Orthogonal prefilters preserving approximation order $p \leq 2$, *IEEE Trans. Circuit Systems II: Analog and Digital Signal Process.* **45** (1998), 1106–1112.
14. J. T. Miller and C.-C. Li, Adaptive multiwavelet initialization, *IEEE Trans. Signal Process.* **46** (1998), 3282–3291.
15. G. G. Walter, A sampling theorem for wavelet subspaces, *IEEE Trans. Inform. Theory* **38** (1992), 881–884.
16. X.-G. Xia and Z. Zhang, On sampling theorem, wavelets, and wavelet transforms, *IEEE Trans. Signal Process.* **41** (1993), 3524–3535.
17. R. M. Lewis, Cardinal interpolating multiresolution, *J. Approx. Theory* **76** (1994), 177–202.
18. J.-K. Zhang and Z. Bao, Three-band compactly supported orthogonal interpolating scaling function, *IEE Electron. Lett.* **34** (1998), 451–452.
19. J.-K. Zhang and Z. Bao, Property of vanishing moments of orthogonal M-band compactly supported orthogonal interpolating scaling function, *IEE Electron. Lett.* **34** (1998), 1917–1918.
20. J.-K. Zhang, “Study on Initialization of Wavelet Series Transform and Theory of M-Band Interpolating Wavelets,” Ph.D. Dissertation, Xidian University, 1999.
21. I. W. Selesnick, Interpolating multiwavelet bases and sampling theorem, *IEEE Trans. Signal Process.* **47** (1999), 1615–1621.
22. W. Sweldens, The lifting scheme: A construction of second generation wavelets, *Appl. Comput. Harmon. Anal.* **3** (1996), 186–200.
23. W. Sweldens, The lifting scheme: A custom-design construction of biorthogonal wavelets, *SIAM J. Math. Anal.* **29** (1997), 511–546.
24. N. Saito and G. Beylkin, Multiresolution representations using the auto-correlation functions of compactly supported wavelets, *IEEE Trans. Signal Process.* **41** (1993), 3584–3590.
25. X.-G. Xia and B. W. Suter, Vector-valued wavelet and vector filter banks, *IEEE Trans. Signal Process.* **44** (1996), 508–518.
26. D. X. Zhou, Interpolatory multiple refinable functions and wavelets, in “Wavelet Applications in Signal and Image Processing VIII,” *Proc. SPIE*, Vol. 4119, San Diego, 2000.
27. M. Vetterli and C. Herley, Wavelets and filter banks: Theory and design, *IEEE Trans. Signal Process.* **40** (1992), 2207–2232.
28. Q. Jiang, On the regularity of matrix refinable functions, *SIAM J. Math. Anal.* **29** (1998), 1157–1176.
29. W. J. Shensa, The discrete wavelet transform: Wedding the à trous and Mallat algorithms, *IEEE Trans. Signal Process.* **40** (1992), 2464–2482.
30. M. Vetterli and J. Kovacevic, “Wavelets and Subband Coding,” Prentice-Hall, Englewood Cliffs, NJ, 1995.
31. P. P. Vaidyanathan, “Multirate Systems and Filter Banks,” Prentice-Hall, Englewood Cliffs, NJ, 1993.
32. G. Strang and T. Nguyen, “Wavelets and Filter Banks,” Wellesley–Cambridge Press, Wellesley, MA, 1995.